

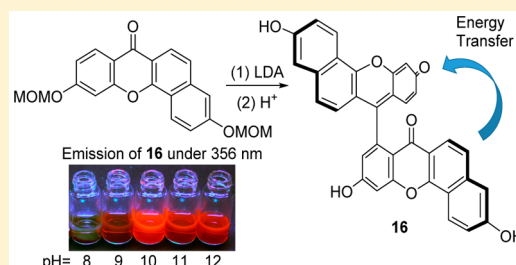
Fluorescent Dyes with Directly Connected Xanthone and Xanthene Units

Akane Katori, Eriko Azuma, Hina Ishimura, Kouji Kuramochi, and Kazunori Tsubaki*

Graduate School of Life and Environmental Sciences, Kyoto Prefectural University, Shimogamo, Sakyo-ku, Kyoto 606-8522, Japan

Supporting Information

ABSTRACT: Unexpected dimerization of a methoxymethyl-protected xanthone occurred upon treatment with an aryl lithium reagent generated from 2-bromo-1,3-dimethylbenzene and *n*-butyllithium. The hydrogen between two directing etheral oxygen atoms was not abstracted, but that adjacent to the carbonyl group was removed to afford a dimeric compound containing two directly connected fluorescent xanthone and xanthene units. Starting from this discovery, three dimeric dyes were constructed, and their optical properties were examined. Although the two fluorescent units were orthogonal in each dye, efficient energy transfer was observed in dimeric dye **16** in three solvent systems. In contrast, solvent-dependent energy transfer was detected for another dimeric dye, **5**. After close investigation, we found that the orientation factor (κ) is the main factor influencing Förster resonance energy transfer in these dyes.



INTRODUCTION

Fluorescent dyes such as fluorescein and rhodamine are essential tools in chemical and molecular biology.¹ Recently, as represented by TokyoGreen,² on/off fluorescent systems using xanthene-based skeletons have been rationally developed through the reaction of the carbonyl groups on xanthone derivatives with aryl metal species. The electronic properties of these systems have been tuned by introducing substituents onto the aryl group (Figure 1).³

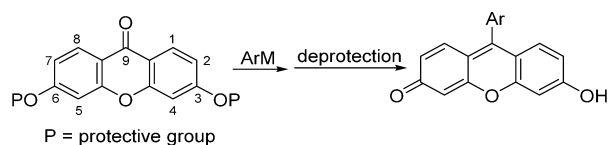


Figure 1. Synthesis of a xanthene dye from the corresponding xanthone.

We have extensively investigated the synthesis of (di)benzoxanthones⁴ and (di)naphthofluoresceins⁵ possessing additional benzene units on one or both sides of xanthone and fluorescein. These compounds showed potential for multicolor fluorescent sensing and exhibited fluorescent emission in the near-infrared region (>700 nm) with large Stokes shifts. During these studies, when we treated methoxymethyl (MOM)-protected xanthone **1**⁶ with the aryl lithium reagent formed from 2-bromo-1,3-dimethylbenzene and *n*-butyllithium (*n*-BuLi) in THF, we noticed that two new fluorescent products were generated along with regular coupling product **2** (10% yield). We isolated these fluorescent products, and subsequent NMR spectroscopic characterization indicated that they have similar frameworks. The spectroscopic data suggested that one was a dimer of xanthone **1** with three

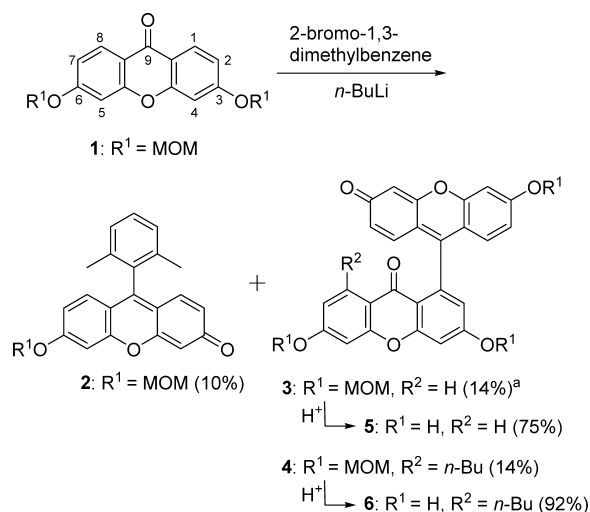
MOM groups and the other was the same dimer framework with an additional butyl group.

Abrams reported that in the direct deuterium labeling of simple xanthone with lithium amide deprotonation first occurred on C-4 of xanthone proximal to the bridged ether oxygen and then on C-1 adjacent to the carbonyl group.⁷ Compared with simple xanthone, **1** has an additional OMOM group on C-3 that could act as a directing group in lithiation. Therefore, we anticipated that lithiation could occur at C-4 and then the lithiated xanthone **1** could react with an unlithiated xanthone **1** to form a dimeric product. In addition, another fluorescent product could be derived by further lithiation at C-5 of the dimeric product and subsequent reaction with bromobutane through halogen–lithium exchange.

However, judging from 2D NMR spectra (COSY, NOESY, HMQC, and HMBC) of the products, the carbonyl group at C-9 clearly acted as a directing group, so the proton at C-1 of xanthone **1** was abstracted by the aryl lithium reagent acting as a base. The xanthone then dimerized to afford compound **3** in 14% yield. A proton at C-8 of dimeric compound **3** was abstracted and trapped by bromobutane to give compound **4** in 14% yield. The three MOM groups in each molecule were then removed without difficulty under acidic conditions to generate compounds **5** (75%) and **6** (92%) from **3** and **4**, respectively (Scheme 1).⁸ Because compound **5** is simply composed of xanthene and xanthone, and is expected to exhibit interesting optical properties caused by the orthogonal arrangement of the two fluorescent units,⁹ we examined **5** and its related dimeric compounds more closely.

Received: March 3, 2015

Published: April 13, 2015

Scheme 1. Unexpected Dimerization of Xanthone 1 Treated with a Bulky Aryl Lithium Reagent^a

^aThe yield of 3 was improved to 61% by using LDA as the base. Refer to the main text for details.

RESULTS AND DISCUSSION

Synthesis of Dimeric Dyes. First, we modified the reaction conditions by using LDA as the base instead of the bulky and more nucleophilic aryl lithium reagent to preferentially obtain the desired dimerization product. Despite changing the base, the target dimerization reaction proceeded without difficulty to afford dimeric product 3 in 61% yield in THF at -78°C . We next applied the dimerization reaction conditions to the series of (di)benzoxanthenes 7–14 depicted in Figure 2.^{4,6}

Surprisingly, among these (di)benzoxanthenes, only compound 9 gave desired dimeric product 15 in 42% yield (Scheme 2). The structure of compound 15 was clarified by 2D NMR spectroscopy. LDA induced deprotonation at C-8 rather than C-6 of compound 9, forming a species that reacted with

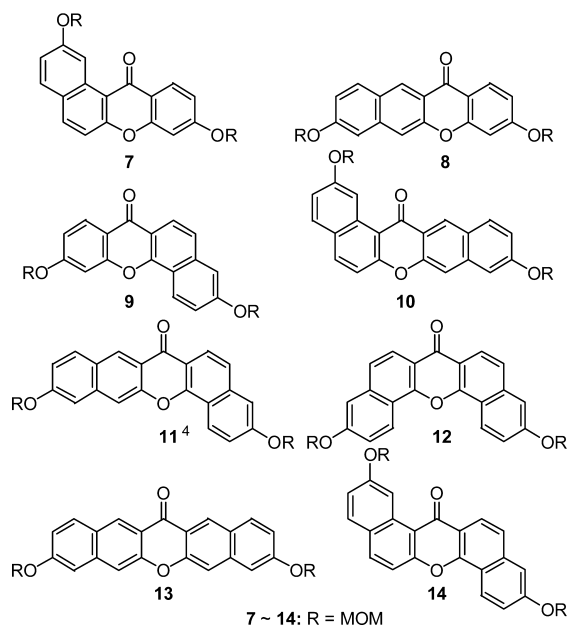
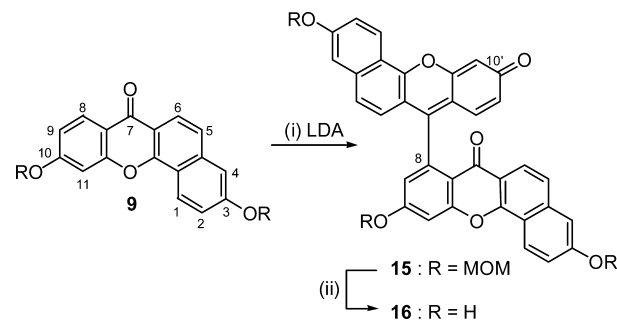


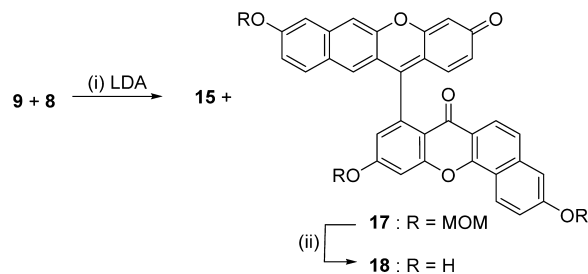
Figure 2. MOM-protected (di)benzoxanthenes 7–14.

Scheme 2. Synthesis of Homodimeric Compound 16^a

^a(i) LDA, THF, 42%. (ii) 4 M HCl, dioxane, 95%.

another 9. Dimerization was followed by dehydration along with removal of the MOM group at C-10' of one xanthone moiety. The xanthone–xanthene dimeric fluorescent dye 16 was formed in 95% yield by deprotection of 15 under acidic conditions.

Because the xanthone–xanthene dimer was expected to behave as a unique energy transfer system from the donor xanthone unit to the acceptor xanthene unit, judging from preliminary fluorescence measurements, we next constructed a heterodimeric compound. We chose compound 9 as a donor unit and compound 8 as an acceptor unit among (di)benzoxanthenes 7–14 because of the overlap of the emission profile of 9 with the absorption profile of 8. A mixture of compounds 9 and 8 (1.2 equiv) was treated with LDA (1.5 equiv) to give expected heterodimer 17 as well as homodimer 15 in respective yields of 22 and 7%. Compound 17 was treated with 4 M hydrochloric acid in dioxane to give desired 18 in 79% yield (Scheme 3).

Scheme 3. Synthesis of Heterodimeric Compound 18^a

^a(i) LDA, THF, 7% (15), 22% (17). (ii) 4 M HCl, dioxane, 79%.

Optical Properties of Dimeric Dyes. With dimeric fluorescent dyes 5, 16, and 18 in hand, we next investigated their optical properties. In particular, we aimed to determine (1) how energy transfer from the donor xanthone unit to the acceptor xanthene unit was affected by their orthogonal arrangement⁹ and (2) the dependence of energy transfer in the dimeric dyes on pH¹⁰ because each dye molecule contained three pH-sensitive phenolic hydroxyl groups.

We measured the UV–vis and fluorescent spectra of 16 in various aqueous buffered media (pH 1–12) to assess its potential for use in bioimaging. Photographs of 16 under UV (365 nm) and natural light as well as its UV–vis and fluorescent spectra are depicted in Figure 3. Dimeric dye 16 had poor solubility in aqueous solution and formed a precipitate under acidic and neutral conditions. In the pH range of 9–12, the highest fluorescence intensity was observed

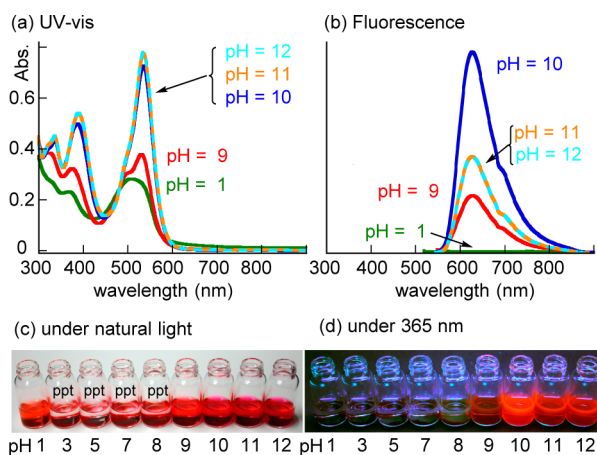


Figure 3. (a) UV-vis and (b) fluorescence spectra of compound **16** under various pH conditions. Photographs of compound **16** at various pH values under (c) natural light and (d) 365 nm UV light. Conditions: [**16**] = 2.0×10^{-5} M for UV-vis and fluorescent measurements. [**16**] = 1.0×10^{-4} M for photographs. HCl-KCl buffer (pH 1), citrate-phosphate buffer (pH 3, 5, 7), Tris-HCl buffer (pH 8, 9), and glycine-NaOH buffer (pH 10, 11, 12). ppt, precipitation.

at pH 10 (Figure 3b), whereas the UV-vis spectra of compound **16** at pH 10–12 were comparable (Figure 3a).

Next, UV-vis and fluorescence spectra of dimeric fluorescent dyes **5**, **16**, and **18** were scrutinized in three different solvent systems, methanol, 8.3×10^{-2} M NaOH in methanol, and glycine-NaOH buffer solution (pH 10). The UV-vis and fluorescence spectra of the corresponding fragments in dimeric dyes were also measured as reference compounds **19**–**23** (Figure 4).^{4,12}

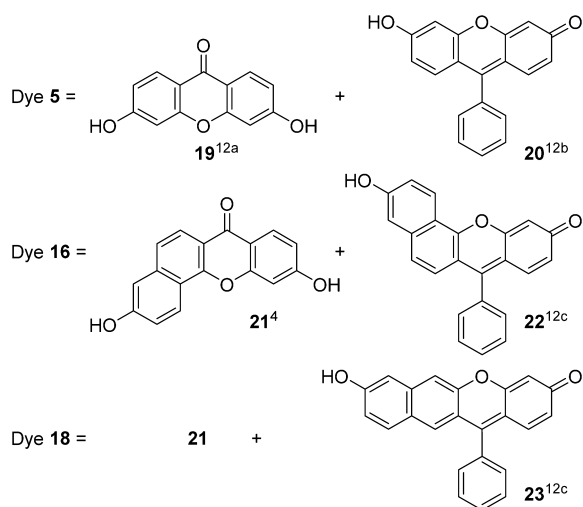


Figure 4. Structures of reference compounds **19**–**23**.

Figure 5 shows the UV-vis and fluorescence spectra of dimeric dye **5** and its fragments **19**^{12a} and **20**^{12b} in the three solvent systems. Focusing on the UV spectra (Figure 5a,c,e), the UV spectrum of **5** is almost the sum of those of constituents **19** and **20** in each medium. Thus, the two fragments of **5** do not interact in the ground state. Regarding the fluorescence spectra (Figure 5b), fragment **19** exhibits a peak at around 429 nm and fragment **20** emits at 518 nm in methanol solution. When the xanthone unit of **5** was irradiated at 316 nm, negligible fluorescence was observed from the xanthone unit at

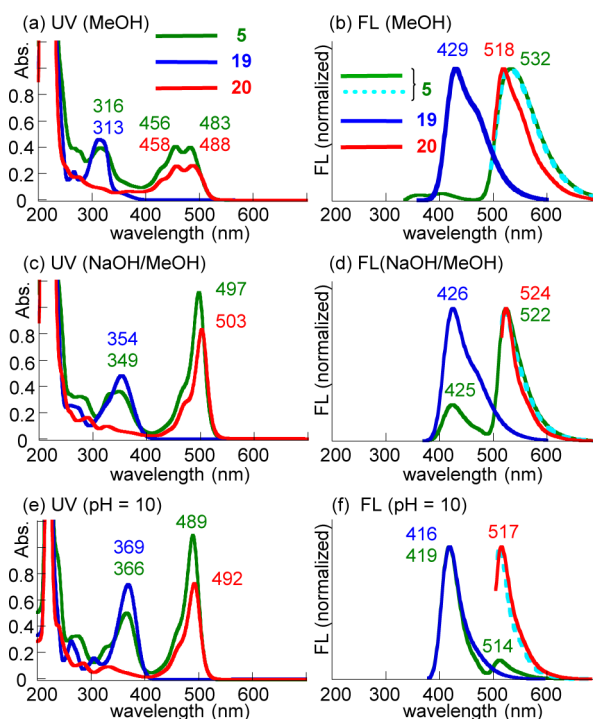


Figure 5. (a, c, e) UV-vis and (b, d, f) fluorescence spectra of dimeric dye **5** and its fragments **19** and **20**. Conditions: [**5**, **19**, **20**] = 2.0×10^{-5} M, (a, b) methanol, (c, d) 8.3×10^{-2} M NaOH/methanol, and (e, f) glycine-NaOH buffer (pH 10), 25 °C; light path length, 1 cm. For fluorescent spectra of dimeric dye **5**, the solid green line indicates excitation of the donor xanthone unit, and the dotted pale blue line indicates excitation of the acceptor xanthene unit.

ca. 420 nm, but considerable fluorescence was exhibited from the xanthene unit at around 532 nm. These data indicate that efficient energy transfer occurred from the xanthone unit as a donor to the xanthene unit as an acceptor. In NaOH/methanol solution (Figure 5d), the efficiency of this energy transfer decreased, and emissions derived from both xanthone (425 nm) and xanthene (522 nm) were observed. Furthermore, the energy transfer between the units was disrupted in buffer solution (Figure 5f). Thus, almost no fluorescence from the xanthone unit occurred through the energy transfer pathway, and each unit acted as an independent fluorophore.

In the case of dimeric dye **16**, additivity of UV spectra was also confirmed in the three solvent systems (Figure 6a,c,e), so no interaction between donor xanthone and acceptor xanthene units was again observed in the ground state. When the donor xanthone unit was excited, the intensity of fluorescence from the acceptor xanthene unit was increased through energy transfer in all three solvent systems.

For heterodimeric dye **18**, the emission from the xanthene unit was very weak, so it is not suitable for use as a fluorescent material (see the Supporting Information).

The optical properties of dimeric dyes **5** and **16** are summarized in Table 1. Here, the quantum yield of the donor unit $\Phi_{(d)}$ was calculated based on the intensity of absorption of the donor xanthone unit and the area of fluorescence from the acceptor xanthene unit, whereas the quantum yield of the acceptor unit $\Phi_{(a)}$ was determined from the absorption and fluorescence of the acceptor xanthene unit. The ratio $\Phi_{(d)}/\Phi_{(a)}$ indicates the efficiency of energy transfer from the xanthone unit to the xanthene one. Because the units of dimer **5** act as

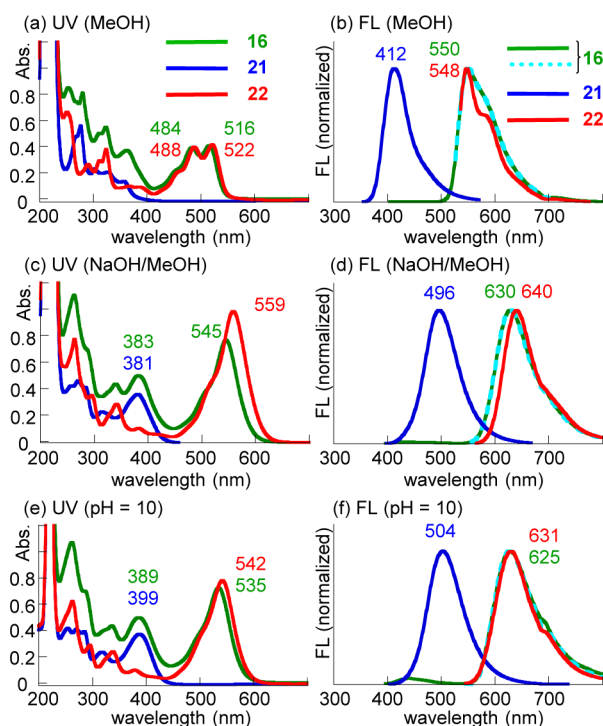


Figure 6. (a, c, e) UV-vis and (b, d, f) fluorescence spectra of dimeric dye **16** and its fragments **21** and **22**. Conditions: [**16**, **21**, **22**] = 2.0×10^{-5} M, (a, b) methanol, (c, d) 8.3×10^{-2} M NaOH/methanol, and (e, f) glycine-NaOH buffer (pH 10), 25 °C; light path length, 1 cm. For fluorescent spectra of dimeric dye **16**, the solid green line indicates excitation of the donor xanthone unit, and dotted pale blue line indicates excitation of the acceptor xanthene unit.

Table 1. Optical Properties of Dimeric Dyes 5 and 16

dye	medium	λ_{abs}	λ_{em}	$\Phi_{(d)}$ (nm) ^a		Δ^c
				$\Phi_{(a)}$ (nm) ^b	$\Phi_{(d)}/\Phi_{(a)}$	
5	MeOH	316	532	0.27 (315)	0.68	216
		483		0.40 (450)		49
	NaOH/MeOH	349	522	0.0062 (360)	0.28	173
		497		0.022 (450)		25
	Buffer (pH 10)	366	514	0.0004 (360)	0.04	148
		489		0.009 (450)		25
16	MeOH	363	550	0.20 (360)	0.77	187
		516		0.26 (450)		34
	NaOH/MeOH	383	630	0.081 (360)	0.54	247
		545		0.15 (540)		85
	Buffer (pH 10)	389	625	0.006 (360)	0.35	236
		535		0.018 (540)		90

^a $\Phi_{(d)}$, quantum yield obtained through the energy transfer pathway following excitation of the donor xanthone unit. $\Phi_{(a)}$, quantum yield of the directly irradiated acceptor xanthene unit. The excitation wavelength λ_{ext} is shown in parentheses. ^bQuantum yields were determined using a solution of quinine sulfate in 1 M H₂SO₄ as a reference standard ($\Phi = 0.56$) for $\lambda_{\text{ext}} = 315\text{--}360$ nm, fluorescein in 0.1 M NaOH as a standard ($\Phi = 0.98$) for $\lambda_{\text{ext}} = 450$ nm, and dinaphthofluorescein¹³ in buffer (pH 10) as a standard ($\Phi = 0.14$) for $\lambda_{\text{ext}} = 540$ nm. ^cDifference between the wavelengths of emission and absorption maxima.

two independent fluorescent dyes, especially in buffer medium, $\Phi_{(d)}/\Phi_{(a)}$ is obviously lower in buffer than in methanol. In contrast, for dimer **16** where the fluorescence did not originate from the donor xanthone unit, relatively high values of $\Phi_{(d)}/\Phi_{(a)}$

$\Phi_{(a)}$, 0.35–0.77, were maintained regardless of the kind of solvent along with very large differences between absorption and emission wavelengths Δ ($\lambda_{\text{em}} - \lambda_{\text{abs}}$) of around 200 nm. The quantum yield Φ of fragment molecule **21** was 28% in methanol,⁴ whereas those of **16** were 20% for irradiation of the donor xanthone and 26% for irradiation of the acceptor xanthene. The resulting $\Phi_{(d)}/\Phi_{(a)}$ of 0.77 in methanol indicates that rapid and effective energy transfer occurs in dimeric dye **16**.

To elucidate the mechanism of effective energy transfer of dimer **5**, the most stable conformations of both the ground and excited states of neutral and monoanionic forms of **5** were estimated using density functional theory (DFT) at the B3LYP/6-31+G level for the ground-state calculations and the configuration interaction singles method (CIS/6-31+G) for the excited-state calculations.¹¹

The optimized structures of **5** are illustrated in Figure 7. The calculated dihedral angle, defined by the four atoms in blue in

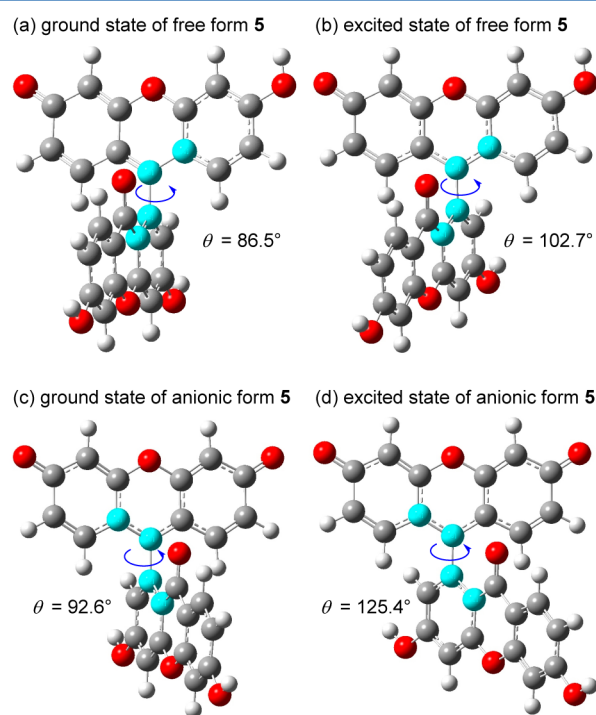


Figure 7. Optimized structures of dimeric compound **5** in ground and excited states. (a) Free form in the ground state, (b) free form in an excited state, (c) anionic form in the ground state, and (d) anionic form in an excited state.

each structure, of the neutral form of **5** in the ground state is 86.5° (Figure 7a), whereas that of the monoanionic form in the ground state is 92.6° (Figure 7c). Thus, the xanthone and xanthene units are orthogonal in the ground state. These data clearly support the additivity of the UV spectra of **5** in the three different solvent systems (Figure 5a,c,e). In contrast, the dihedral angles of the excited states of free and anionic **5** increased to 102.7° and 125.4°, respectively. Because the two fluorophore units in **5** are not orthogonal in the excited state, it is unsurprising that effective energy transfer was observed in methanol. We should rather examine why emissions derived from both xanthone and xanthene were observed from dimeric dye **5** in basic methanol and why fluorescence originated from only the donor xanthone in **5** in basic buffer medium.

A simplified Jablonski diagram (Figure 8) reveals that after vertical excitation and internal conversion, electrons in the excited S_{1D} state relax back to the ground state S_{0D} mainly through nonradiative relaxation, fluorescence, and energy transfer, which have rates of k_{nrD} , k_{fD} , and $k_{T(r)}$, respectively.¹⁴ When k_{fD} is sufficiently larger than $k_{T(r)}$, fluorescence from the donor will be observed. Conversely, if $k_{T(r)} \gg k_{fD}$, then fluorescence from the acceptor will be predominant, and if $k_{T(r)} \approx k_{fD}$, then fluorescence from both the donor and acceptor will be observed.

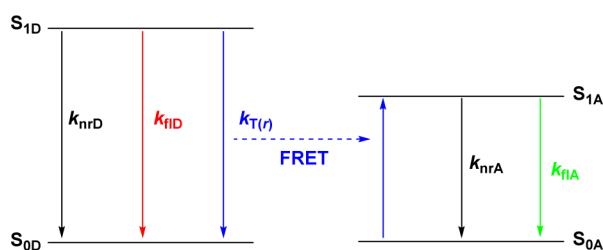


Figure 8. Simplified Jablonski diagram. k_{nrD} , rate of nonradiative decay from the donor; k_{fD} , rate of fluorescence from the donor; $k_{T(r)}$, rate of energy transfer; k_{nrA} , rate of nonradiative decay from the acceptor; and k_{fA} , rate of fluorescence from the acceptor.

In the Förster resonance energy transfer mechanism, the rate of energy transfer $k_{T(r)}$ is given as follows^{14a}

$$k_{T(r)} = \frac{Q_D \kappa^2}{\tau_D r^6} \left[\frac{9000(\ln 10)}{128\pi^5 n^4 N_A} \right] \int_0^\infty F_D(\lambda) \varepsilon_A(\lambda) \lambda^4 d\lambda \quad (1)$$

where Q_D is the quantum yield of the donor in the absence of the acceptor, κ is the orientation of the donor emission dipole moment with respect to that of the acceptor absorption dipole moment, τ_D is the fluorescent lifetime of the donor, r is the distance between donor and acceptor units, n is the refractive index of the medium, N_A is Avogadro's number, and the integral term indicates the overlap of the donor emission spectrum with the absorption spectrum of the acceptor.

Because k_{fD} is constant under the given conditions, $k_{T(r)}$ plays an important role in determining the dominant relaxation process. Thus, to explain the fluorescent behavior of dimer **5** in various solvent systems (Figure 5), its $k_{T(r)}$ in methanol should be vastly greater than that in basic aqueous medium. On the basis of this idea, the individual terms in eq 1 were scrutinized. Measured and calculated values of individual terms are as follows; Q_D (quantum yield of fragment **19**) is 0.32 in methanol and 0.73 in buffer (pH 10), τ_D (fluorescent lifetime of fragment **19**) is 4.4 ns in methanol and 2.8 ns in buffer (pH 10), r is constant in this case, and n^4 is 3.12 in methanol¹⁵ and 3.16 in water.¹⁶ These terms accordingly show the limited influence of $k_{T(r)}$ on the fluorescence of **5**. For the integral term in eq 1, the overlap between the emission of the donor xanthone unit and absorption of the acceptor xanthene unit of dimer dye **5** partially depended on the solvent system. The emission ascribed to the donor xanthone unit shifted to shorter wavelength when the solvent was changed from methanol to buffer; the emission from xanthone fragment **19** appeared at 429 nm in methanol, 426 nm in NaOH/methanol, and 416 nm in basic buffer. Meanwhile, the absorbance of the acceptor xanthene moved to longer wavelength, with the absorbance from xanthene fragment **20** appearing at 458 and 488 nm in

methanol, 503 nm in NaOH/methanol, and 492 nm in buffer. Although these shifts may be used to interpret the larger $k_{T(r)}$ in methanol than in basic aqueous medium, there is still sufficient overlap of the emission and absorption peaks to allow energy transfer. Therefore, the integral term is not a deciding factor of $k_{T(r)}$. Through elimination of other factors, we find that κ should be an important parameter determining the likelihood of energy transfer. As the medium becomes basic and phenolic hydroxyl groups become phenolate and/or the water content increases, the dihedral angle between xanthone and xanthene moieties becomes orthogonal. If two dipole moments are orthogonal, in principle, energy transfer from donor to acceptor should not be observed. This interpretation seemingly contradicts the results of the DFT calculations depicted in Figure 7. However, the DFT calculation gives the most stable conformation of the S1 state of an individual molecule in vacuum at absolute zero, whereas in real systems, the interactions between excited dimers and polar water molecules are not negligible. In the case of dimeric dye **16**, even though the two aromatic rings are orthogonal, the corresponding dipole moment is at an angle to the aromatic rings, so the scalar product of the dipole moments is not zero.

The above consideration is supported by the fluorescence lifetime (τ) of dimer dye **5** calculated by considering the excitation and emission of the donor unit and its fragment **19** (Table 2). In methanol, because the fluorescence from the

Table 2. Fluorescence Lifetimes (τ , 10^{-9} s) of Dimer **5** and Its Fragment **19** Based on the Excitation and Emission of Xanthone Units

compound	5	19
Methanol	3.8, 1.2 ^a	4.4 ^a
NaOH/methanol	4.0, 1.7 ^a	3.7 ^a
Buffer (pH 10)	2.8 ^b	2.8 ^c

^a $\lambda_{ex} = 295$ nm, $\lambda_{em} = 429$ nm. ^b $\lambda_{ex} = 295$ nm, $\lambda_{em} = 419$ nm. ^c $\lambda_{ex} = 295$ nm, $\lambda_{em} = 416$ nm.

donor xanthone fragment of **5** was quite weak, τ was calculated using a low photon count. In methanol and NaOH/methanol solvent systems, in which energy transfer from xanthone to xanthene units in dimer dye **5** was observed, two-component τ of 3.8 and 1.2 ns in methanol and 4.0 and 1.7 ns in NaOH/methanol were determined. On the basis of comparison with τ of the donor fragment **19** (4.4 ns in methanol and 3.7 ns in NaOH/methanol), the shorter component was ascribed to the energy transfer process.

CONCLUSIONS

We described the synthesis of novel xanthone and xanthene dimeric dyes and examined their optical properties in three solvent systems. In dimeric dye **16**, effective energy transfer between units was observed in all three solvent systems despite their orthogonal conformation. In contrast, energy transfer in dimeric dye **5** was affected by the solvent system. We believe that this difference is caused by κ in the Förster equation. Studies to develop fluorescent dyes with high quantum yield and large Δ ($\lambda_{em} - \lambda_{abs}$) based on orthogonal dimeric dye skeletons are currently in progress.

EXPERIMENTAL SECTION

Synthesis of Dimeric Compounds from MOM-Protected Xanthone and Aryl Lithium (Figure 1). A solution of *n*-BuLi (1.60

M *n*-hexane solution; 0.395 mL, 0.632 mmol) was added dropwise to a solution of 2-bromo-1,3-dimethylbenzene (88 μ L, 0.664 mmol) in dry THF (4 mL) under a N₂ atmosphere at -78°C . After stirring for 105 min, a solution of **1** (100 mg, 0.316 mmol) in dry THF (3 mL) was added dropwise at same temperature. After 50 min, the reaction solution was warmed to room temperature and stirred for a further 50 min. The reaction mixture was poured into ethyl acetate and water. The organic layer was successively washed with water twice and then brine, dried over Na₂SO₄, filtered, and concentrated under reduced pressure. The residue was purified by column chromatography (SiO₂; *n*-hexane/AcOEt = 5:1 \rightarrow 1:1) to afford **2** (11.2 mg, 10% yield), dimeric compound **3** (12.8 mg, 14% yield), and compound **4** (13.7 mg, 14% yield).

9-(2,6-Dimethylphenyl)-6-(methoxymethoxy)xanthen-3-one (2). Yield 10%; brown oil; IR (neat) 2956, 2929, 2362, 1641, 1598, 1151, 1153, 1078 cm⁻¹; ¹H NMR (400 MHz, CDCl₃) δ 7.35 (t, *J* = 7.6 Hz, 1H), 7.21 (d, *J* = 7.6 Hz, 2H), 7.18 (d, *J* = 2.0 Hz, 1H), 6.94 (d, *J* = 8.8 Hz, 1H), 6.89 (d, *J* = 9.6 Hz, 1H), 6.86 (dd, *J* = 8.8 Hz, 2.0 Hz, 1H), 6.58 (dd, *J* = 9.6 Hz, 2.0 Hz, 1H), 6.46 (d, *J* = 2.0 Hz, 1H), 5.28 (s, 2H), 3.52 (s, 3H), 2.00 (s, 6H); ¹³C NMR (100 MHz, CDCl₃) δ 185.9, 161.8, 158.4, 154.5, 149.1, 136.0, 132.0, 130.6, 130.0, 129.2, 128.6, 127.8, 118.5, 114.5, 114.4, 105.9, 103.3, 94.4, 56.5, 19.8; HRMS (EI⁺, double-focusing magnetic sector) calcd for C₂₃H₂₁O₄ (M + H)⁺, 361.1430; found, 361.1440.

1-Butyl-3,6-bis(methoxymethoxy)-8-[3-(methoxymethoxy)-6-oxo-xanthen-9-yl]xanthen-9-one (4). Yield 14%; yellow solid; mp 63–66 $^{\circ}\text{C}$; IR (KBr) 2960, 1643, 1598, 1550, 1518, 1444, 1375 cm⁻¹; ¹H NMR (400 MHz, CDCl₃) δ 7.25 (d, *J* = 2.4 Hz, 1H), 7.18 (d, *J* = 2.4 Hz, 1H), 6.97 (d, *J* = 8.8 Hz, 1H), 6.97 (d, *J* = 9.6 Hz, 1H), 6.96 (d, *J* = 2.4 Hz, 1H), 6.79 (dd, *J* = 8.8 Hz, 2.4 Hz, 1H), 6.78 (d, *J* = 2.4 Hz, 1H), 6.71 (d, *J* = 2.4 Hz, 1H), 6.54 (dd, *J* = 9.6 Hz, 2.0 Hz, 1H), 6.49 (d, *J* = 2.0 Hz, 1H), 5.31 (s, 2H), 5.27 (s, 2H), 5.26 (s, 2H), 3.54 (s, 3H), 3.51 (s, 3H), 3.49 (s, 3H), 3.06–2.92 (m, 2H), 1.28–1.11 (m, 4H), 0.69 (t, *J* = 7.2 Hz, 3H); ¹³C NMR (100 MHz, CDCl₃) δ 185.8, 175.4, 161.2, 160.9, 160.8, 159.2, 158.9, 157.5, 153.9, 151.1, 148.8, 135.0, 130.4, 129.6, 128.6, 117.3, 117.2, 116.1, 115.8, 115.7, 114.6, 113.9, 105.6, 103.9, 103.1, 101.0, 94.7, 94.4, 94.2, 56.7, 56.4, 56.4, 34.7, 33.2, 22.4, 13.8; HRMS (EI⁺, double-focusing magnetic sector) calcd for C₃₆H₃₅O₁₀ (M + H)⁺, 627.2236; found, 627.2230.

General Procedure To Protect Hydroxy Groups with MOMCl. The following preparation of a MOM-protected xanthone is typical. To a stirred solution of 3,6-dihydroxyxanthone (2.10 g, 9.20 mmol) in dry DMF (20 mL) cooled in an ice bath was added NaH (60% dispersion in mineral oil, 0.92 g, 23.0 mmol, 2.5 equiv) portionwise. After 15 min, MOMCl (1.5 mL, 20.2 mmol, 2.2 equiv) was added dropwise, and then the mixture was stirred for 2 h at room temperature. The reaction mixture was poured into ethyl acetate and water. The organic layer was separated and washed with water three times and then brine. After being dried over sodium sulfate, the solvent was evaporated in vacuo to give a residue. The residue was washed with *n*-hexane to afford **1** (2.83 g, 97%) as a white powder.

3,6-Bis(methoxymethoxy)xanthen-9-one (1). Yield 97%; white powder; mp 158–161 $^{\circ}\text{C}$; IR (KBr) 3079, 3002, 2964, 2900, 2844, 2821, 2792, 1614, 1569, 1442, 1313, 1253, 1220, 1157, 1078 cm⁻¹; ¹H NMR (400 MHz, CDCl₃) δ 8.23 (d, *J* = 8.8 Hz, 2H), 7.05 (d, *J* = 2.4 Hz, 2H), 7.01 (dd, *J* = 8.8 Hz, 2.4 Hz, 2H), 5.28 (s, 4H), 3.51 (s, 6H); ¹³C NMR (100 MHz, CDCl₃) δ 175.5, 162.1, 157.7, 128.1, 116.5, 113.8, 103.0, 94.3, 56.3; HRMS (FT-ICR-MS) calcd for C₁₇H₁₆O₆Na (M + Na)⁺, 339.0851; found, 339.0839.

2,9-Bis(methoxymethoxy)benzo[a]xanthen-12-one (7). Yield 80%; white powder; mp 110–111 $^{\circ}\text{C}$; IR (KBr) 2998, 2956, 2898, 2825, 1619, 1594, 1515, 1448, 1349, 1265, 1155, 1074, 1004, 919 cm⁻¹; ¹H NMR (400 MHz, CDCl₃) δ 9.82 (d, *J* = 2.4 Hz, 1H), 8.35 (d, *J* = 9.2 Hz, 1H), 8.03 (d, *J* = 8.8 Hz, 1H), 7.81 (d, *J* = 8.8 Hz, 1H), 7.39 (d, *J* = 8.8 Hz, 1H), 7.32 (dd, *J* = 9.2 Hz, 2.4 Hz, 1H), 7.15 (d, *J* = 2.4 Hz, 1H), 7.09 (dd, *J* = 8.8 Hz, 2.4 Hz, 1H), 5.45 (s, 2H), 5.31 (s, 2H), 3.58 (s, 3H), 3.54 (s, 3H); ¹³C NMR (100 MHz, CDCl₃) δ 177.7, 161.6, 158.0, 156.0, 135.7, 132.6, 129.6, 128.0, 125.7, 118.1, 117.8, 115.5, 114.4, 113.7, 110.0, 102.4, 94.5, 94.3, 56.5, 56.3 (one

peak overlapped); HRMS (FT-ICR-MS) calcd for C₂₁H₁₈O₆Na (M + Na)⁺, 389.1004; found, 389.0996.

3,8-Bis(methoxymethoxy)benzo[b]xanthen-12-one (8). Yield 71%; white powder; mp 166–168 $^{\circ}\text{C}$; IR (KBr) 3052, 2958, 2900, 2823, 1658, 1621, 1469, 1438, 1392, 1326, 1251, 1155, 1002, 916 cm⁻¹; ¹H NMR (400 MHz, CDCl₃) δ 8.78 (s, 1H), 8.25 (d, *J* = 8.8 Hz, 1H), 7.94 (d, *J* = 8.8 Hz, 1H), 7.65 (s, 1H), 7.36 (d, *J* = 2.4 Hz, 1H), 7.19 (d, *J* = 8.8 Hz, 2.4 Hz, 1H), 7.06 (d, *J* = 2.4 Hz, 1H), 6.99 (dd, *J* = 8.8 Hz, 2.4 Hz, 1H), 5.33 (s, 2H), 5.30 (s, 2H), 3.54 (s, 3H), 3.53 (s, 3H); ¹³C NMR (100 MHz, CDCl₃) δ 176.8, 162.7, 158.2, 157.4, 153.0, 138.0, 131.4, 128.5, 127.9, 125.8, 119.7, 119.4, 115.9, 113.4, 112.1, 107.8, 103.0, 94.3, 94.3, 56.4, 56.3; HRMS (FT-ICR-MS) calcd for C₂₁H₁₈O₆Na (M + Na)⁺, 389.1005; found, 389.0996.

3,10-Bis(methoxymethoxy)benzo[c]xanthen-7-one (9). Yield 94%; light brown powder; mp 169–171 $^{\circ}\text{C}$; IR (KBr) 2956, 2900, 1654, 1614, 1569, 1471, 1421, 1369, 1238, 1193, 1159, 1072, 995 cm⁻¹; ¹H NMR (400 MHz, CDCl₃) δ 8.54 (d, *J* = 9.2 Hz, 1H), 8.30 (d, *J* = 8.8 Hz, 1H), 8.22 (d, *J* = 8.8 Hz, 1H), 7.61 (d, *J* = 8.8 Hz, 1H), 7.46 (d, *J* = 2.4 Hz, 1H), 7.38 (dd, *J* = 9.2 Hz, 2.4 Hz, 1H), 7.28 (d, *J* = 2.4 Hz, 1H), 7.08 (dd, *J* = 8.8 Hz, 2.4 Hz, 1H), 5.35 (s, 2H), 5.34 (s, 2H), 3.55 (s, 3H), 3.55 (s, 3H); ¹³C NMR (100 MHz, CDCl₃) δ 176.6, 162.0, 158.0, 157.2, 153.8, 138.2, 128.0, 124.0, 123.2, 122.3, 119.2, 119.1, 117.1, 116.3, 114.6, 110.5, 103.1, 94.4, 94.4, 56.4, 56.3; HRMS (FT-ICR-MS) calcd for C₂₁H₁₈O₆Na (M + Na)⁺, 389.1008; found, 389.0996.

2,10-Bis(methoxymethoxy)dibenzo[a,i]xanthen-14-one (10). Yield 52%; brown powder; mp 175–178 $^{\circ}\text{C}$; IR (KBr) 2952, 2923, 2852, 2827, 1650, 1623, 1515, 1473, 1444, 1351, 1268, 1151, 1079, 998 cm⁻¹; ¹H NMR (400 MHz, CDCl₃) δ 9.81 (d, *J* = 2.4 Hz, 1H), 8.92 (s, 1H), 8.06 (d, *J* = 8.8 Hz, 1H), 7.99 (d, *J* = 9.2 Hz, 1H), 7.81 (d, *J* = 8.8 Hz, 1H), 7.78 (s, 1H), 7.43 (d, *J* = 9.2 Hz, 1H), 7.42 (s, 1H), 7.31 (dd, *J* = 8.8 Hz, 2.4 Hz, 1H), 7.23 (dd, *J* = 8.8 Hz, 2.4 Hz, 1H), 5.46 (s, 2H), 5.35 (s, 2H), 3.60 (s, 3H), 3.56 (s, 3H); ¹³C NMR (100 MHz, CDCl₃) δ 179.2, 158.8, 158.4, 157.3, 151.9, 137.8, 136.6, 132.9, 131.5, 129.9, 127.9, 126.2, 125.7, 121.3, 119.6, 117.8, 115.9, 113.0, 111.9, 110.1, 107.8, 94.6, 94.3, 56.6, 56.3; HRMS (FT-ICR-MS) calcd for C₂₅H₂₀O₆Na (M + Na)⁺, 439.1166; found, 439.1152.

Compound 11. Known.⁴

3,11-Bis(methoxymethoxy)dibenzo[c,h]xanthen-7-one (12). Yield 78%; pale pink powder; mp 179–181 $^{\circ}\text{C}$; IR (KBr) 2956, 2850, 2829, 1639, 1569, 1471, 1421, 1367, 1240, 1205, 1153, 1079, 1004, 925 cm⁻¹; ¹H NMR (400 MHz, CDCl₃) δ 8.55 (d, *J* = 8.8 Hz, 2H), 8.20 (d, *J* = 8.8 Hz, 2H), 7.58 (d, *J* = 8.8 Hz, 2H), 7.41 (d, *J* = 2.0 Hz, 2H), 7.36 (dd, *J* = 8.8 Hz, 2.0 Hz, 2H), 5.33 (s, 4H), 3.54 (s, 6H); ¹³C NMR (100 MHz, CDCl₃) δ 176.1, 157.8, 152.9, 138.0, 124.2, 123.6, 122.2, 119.3, 119.3, 117.0, 110.5, 94.4, 56.3; HRMS (FT-ICR-MS) calcd for C₂₅H₂₀O₆Na (M + Na)⁺, 439.1157; found, 439.1152.

3,9-Bis(methoxymethoxy)dibenzo[b,i]xanthen-13-one (13). Yield 83%; yellow powder; mp 206–208 $^{\circ}\text{C}$; IR (KBr) 2954, 2923, 2854, 2827, 1666, 1627, 1498, 1467, 1440, 1932, 1180, 1155, 1079, 1006 cm⁻¹; ¹H NMR (400 MHz, CDCl₃) δ 8.84 (s, 2H), 7.96 (d, *J* = 9.2 Hz, 2H), 7.70 (s, 2H), 7.38 (d, *J* = 2.4 Hz, 2H), 7.20 (dd, *J* = 9.2 Hz, 2.4 Hz, 2H), 5.35 (s, 4H), 3.56 (s, 6H); ¹³C NMR (100 MHz, CDCl₃) δ 178.1, 157.5, 153.0, 138.5, 131.5, 128.2, 125.4, 119.2, 119.1, 111.8, 107.7, 94.2, 56.3; HRMS (FT-ICR-MS) calcd for C₂₅H₂₀O₆Na (M + Na)⁺, 439.1160; found, 439.1152.

2,10-Bis(methoxymethoxy)dibenzo[a,h]xanthen-14-one (14). Yield 85%; brown powder; mp 155–158 $^{\circ}\text{C}$; IR (KBr) 2925, 2580, 2825, 1639, 1600, 1515, 1475, 1524, 1367, 1230, 1153, 1074, 1006 cm⁻¹; ¹H NMR (400 MHz, CDCl₃) δ 9.86 (d, *J* = 2.0 Hz, 1H), 8.54 (d, *J* = 9.2 Hz, 1H), 8.31 (d, *J* = 8.8 Hz, 1H), 8.04 (d, *J* = 9.2 Hz, 1H), 7.81 (d, *J* = 8.8 Hz, 1H), 7.63 (d, *J* = 9.2 Hz, 1H), 7.54 (d, *J* = 8.8 Hz, 1H), 7.45 (d, *J* = 2.0 Hz, 1H), 7.37 (dd, *J* = 9.2 Hz, 2.0 Hz, 1H), 7.31 (dd, *J* = 8.8 Hz, 2.0 Hz, 1H), 5.46 (s, 2H), 5.33 (s, 2H), 3.60 (s, 3H), 3.55 (s, 3H); ¹³C NMR (100 MHz, CDCl₃) δ 178.2, 158.1, 157.9, 157.5, 152.0, 137.8, 135.6, 132.6, 129.7, 126.0, 124.3, 123.6, 122.4, 119.1, 118.9, 118.2, 118.2, 115.6, 114.5, 110.6, 110.2, 94.5, 94.4, 56.6, 56.3; HRMS (FT-ICR-MS) calcd for C₂₅H₂₀O₆Na (M + Na)⁺, 439.1152; found, 439.1152.

General Procedure To Prepare Dimeric Compounds. The following preparation of a dimeric compound **3** is typical. A solution of LDA (1.5 M diethyl ether solution; 0.24 mL, 0.237 mmol) was added dropwise to a solution of **1** (150 mg, 0.474 mmol) in dry THF (5 mL) under a N₂ atmosphere at -78 °C. After stirring for 5 min, the reaction solution was warmed to 0 °C for 15 min. Then, the reaction solution was cooled at -78 °C for 2 h. The reaction mixture was poured into ethyl acetate and water. The organic layer was successively washed with water twice and brine, dried over Na₂SO₄, filtered, and concentrated under reduced pressure to dryness. The residue was purified by column chromatography (SiO₂; *n*-hexane/AcOEt = 5:1 → 2:1) to afford **3** (82.7 mg, 61% yield) as an orange amorphous solid.

3,6-Bis(methoxymethoxy)-1-[3-(methoxymethoxy)-6-oxo-xanthen-9-yl]xanthen-9-one (3). Yield 61%; orange amorphous; mp 85–88 °C; IR (KBr) 2956, 2829, 1643, 1600, 1519, 1477, 1444, 1376, 1301, 1263, 1205, 1155, 1078, 991 cm⁻¹; ¹H NMR (400 MHz, CDCl₃) δ 7.96 (d, *J* = 8.8 Hz, 1H), 7.33 (d, *J* = 2.4 Hz, 1H), 7.18 (d, *J* = 2.4 Hz, 1H), 7.12 (d, *J* = 2.4 Hz, 1H), 6.97 (dd, *J* = 8.8 Hz, 2.4 Hz, 1H), 6.93 (d, *J* = 8.8 Hz, 1H), 6.90 (d, *J* = 9.6 Hz, 1H), 6.83 (d, *J* = 2.4 Hz, 1H), 6.79 (dd, *J* = 8.8, 2.4 Hz, 1H), 6.53 (dd, *J* = 9.6, 2.0 Hz, 1H), 6.49 (d, *J* = 2.0 Hz, 1H), 5.34 (s, 2H), 5.29 (s, 2H), 5.25 (s, 2H), 3.56 (s, 3H), 3.51 (s, 3H), 3.49 (s, 3H); ¹³C NMR (100 MHz, CDCl₃) δ 185.9, 174.2, 162.6, 161.4, 161.3, 159.1, 158.7, 157.2, 153.8, 150.4, 135.4, 130.3, 129.8, 128.5, 128.3, 117.6, 116.4, 116.3, 115.7, 115.4, 114.4, 114.1, 105.0, 104.4, 103.3, 102.8, 94.7, 94.4, 56.8, 56.4, 56.4; HRMS (FT-ICR-MS) calcd for C₃₂H₂₆O₁₀Na (M + Na)⁺, 593.1399; found, 593.1418.

3,10-Bis(methoxymethoxy)-8-[3-(methoxymethoxy)-10-oxo-benzo[*c*]xanthen-7-yl]benzo[*c*]xanthen-7-one (15). Yield 42%. red oil; mp 224–226 °C; IR (KBr) 3072, 2956, 2902, 2827, 1618, 1521, 1477, 1417, 1367, 1245, 1153, 1078, 991 cm⁻¹; ¹H NMR (400 MHz, CDCl₃) δ 8.63 (d, *J* = 9.2 Hz, 2H), 7.89 (d, *J* = 8.8 Hz, 1H), 7.89 (d, *J* = 2.4 Hz, 1H), 7.54 (d, *J* = 8.8 Hz, 1H), 7.46–7.37 (m, 5H), 7.04 (d, *J* = 9.6 Hz, 1H), 6.97 (d, *J* = 8.8 Hz, 1H), 6.94 (d, *J* = 2.0 Hz, 1H), 6.71 (d, *J* = 2.0 Hz, 1H), 6.64 (dd, *J* = 9.6 Hz, 2.0 Hz, 1H), 5.41 (s, 2H), 5.36 (s, 2H), 5.33 (s, 2H), 3.61 (s, 3H), 3.55 (s, 3H), 3.53 (s, 3H); ¹³C NMR (100 MHz, acetone-*d*₆) δ 184.9, 175.0, 162.4, 159.7, 159.3, 159.0, 154.1, 151.3, 149.3, 139.3, 138.2, 136.2, 131.1, 130.9, 125.4, 125.0, 124.6, 124.4, 124.3, 122.5, 120.8, 120.5, 119.6, 119.4, 119.2, 117.6, 117.1, 116.8, 116.4, 111.5, 111.3, 105.7, 105.6, 95.6, 95.1, 56.9, 56.4, 56.4 (two peaks overlapped); HRMS (FT-ICR-MS) calcd for C₄₀H₃₀O₁₀Na (M + Na)⁺, 693.1726; found, 693.1731.

3,10-Bis(methoxymethoxy)-8-[8-(methoxymethoxy)-3-oxo-benzo[*b*]xanthen-12-yl]benzo[*c*]xanthen-7-one (17). Yield 22%. orange oil; mp 166–169 °C; IR (KBr) 3203, 3062, 2952, 2904, 1623, 1602, 1533, 1475, 1415, 1367, 1249, 1147, 1076, 991 cm⁻¹; ¹H NMR (400 MHz, CDCl₃) δ 8.64 (d, *J* = 9.2 Hz, 1H), 7.90 (d, *J* = 8.8 Hz, 1H), 7.72 (s, 1H), 7.61 (d, *J* = 2.4 Hz, 1H), 7.54 (d, *J* = 8.8 Hz, 1H), 7.54 (d, *J* = 9.2 Hz, 1H), 7.46–7.42 (m, 2H), 7.40 (s, 1H), 7.36 (d, *J* = 2.4 Hz, 1H), 7.05 (dd, *J* = 9.2 Hz, 2.4 Hz, 1H), 6.97 (d, *J* = 2.4 Hz, 1H), 6.93 (d, *J* = 9.2 Hz, 1H), 6.48–6.45 (m, 2H), 5.42 (s, 2H), 5.35 (s, 2H), 5.30 (s, 2H), 3.62 (s, 3H), 3.55 (s, 3H), 3.51 (s, 3H); ¹³C NMR (100 MHz, CDCl₃) δ 186.6, 174.5, 161.3, 158.8, 158.3, 158.3, 157.4, 153.4, 149.5, 149.4, 138.4, 137.3, 135.4, 130.8, 130.5, 129.7, 127.9, 126.2, 124.5, 123.8, 122.1, 120.0, 119.5, 119.0, 118.9, 117.1, 116.5, 116.2, 111.5, 110.7, 108.4, 106.6, 104.6, 94.9, 94.2, 94.3, 56.9, 56.4, 56.3 (one peak overlapped); HRMS (FT-ICR-MS) calcd for C₄₀H₃₀O₁₀Na (M + Na)⁺, 693.1717; found, 693.1731.

General Procedure for the Deprotection of MOM Groups. The following deprotection reaction is typical. A solution of 4 M hydrochloric acid in 1,4-dioxane (0.4 mL) was added dropwise to a solution of **3** (26.6 mg, 47.8 μmol) in 1,4-dioxane (0.36 mL) and stirred for 2.5 h at room temperature. The reaction mixture was evaporated in vacuo to give a residue. The residue was washed with *n*-hexane/EtOAc = 10:1 to give **5** as a yellow powder (75% yield).

3,6-Dihydroxy-1-(3-hydroxy-6-oxo-xanthen-9-yl)xanthen-9-one (5). Yield 75%; yellow powder; mp > 300 °C; IR (KBr) 3461, 3432, 3401, 3218, 1608, 1455, 1392, 1294, 1207, 1178, 1116, 848 cm⁻¹; ¹H NMR (400 MHz, methanol-*d*₄) δ 7.67 (d, *J* = 8.8 Hz, 1H), 7.50 (d, *J* = 9.2 Hz, 2H), 7.27 (d, *J* = 1.6 Hz, 2H), 7.16 (d, *J* = 2.0 Hz, 1H), 7.07

(dd, *J* = 9.2 Hz, 1.6 Hz, 2H), 6.88 (d, *J* = 2.0 Hz, 1H), 6.81 (d, *J* = 2.0 Hz, 1H), 6.77 (dd, *J* = 8.8 Hz, 2.0 Hz, 1H); ¹³C NMR (100 MHz, methanol-*d*₄) δ 175.7, 182.6, 170.4, 166.1, 164.5, 160.6, 160.5, 159.6, 134.8, 134.0, 128.8, 121.1, 118.1, 116.7, 115.4, 115.0, 114.8, 105.6, 103.4, 103.3; HRMS (FT-ICR-MS) calcd for C₂₆H₁₄O₇Na (M + Na)⁺, 461.0638; found, 461.0632.

1-Butyl-3,6-dihydroxy-8-(3-hydroxy-6-oxo-xanthen-9-yl)-xanthen-9-one (6). Yield 92%; yellow powder; mp > 300 °C; IR (KBr) 3432, 1604, 1538, 1455, 1392, 1286, 1178, 850, 671 cm⁻¹; ¹H NMR (400 MHz, methanol-*d*₄) δ 7.63 (d, *J* = 9.2 Hz, 2H), 7.36 (d, *J* = 2.4 Hz, 2H), 7.16 (dd, *J* = 9.2 Hz, 2.4 Hz, 2H), 7.12 (d, *J* = 2.4 Hz, 1H), 6.78 (d, *J* = 2.4 Hz, 1H), 6.74 (d, *J* = 2.4 Hz, 1H), 6.54 (d, *J* = 2.4 Hz, 1H), 2.82 (t, *J* = 7.2 Hz, 2H), 1.13–1.05 (m, 4H), 0.64 (t, *J* = 7.2 Hz, 3H); ¹³C NMR (125 MHz, DMSO-*d*₆) δ 174.6, 172.0, 162.2, 162.0, 158.8, 157.1, 157.0, 147.4, 133.8, 131.4, 120.5, 115.3, 115.3, 115.1, 114.7, 111.6, 103.3, 102.5, 100.5, 33.8, 32.7, 21.7, 13.4 (one peak overlapped); HRMS (EI⁺, double-focusing magnetic sector) calcd for C₃₀H₂₃O₇ (M + H)⁺, 495.1451; found, 495.1444.

3,10-Dihydroxy-8-(3-hydroxy-10-oxo-benzo[*c*]xanthen-7-yl)-benzo[*c*]xanthen-7-one (16). Yield 95%; red powder; mp > 300 °C; IR (KBr) 3467, 3052, 2929, 1635, 1604, 1477, 1432, 1405, 1303, 1259, 1172 cm⁻¹; ¹H NMR (400 MHz, methanol-*d*₄) δ 8.82 (d, *J* = 9.2 Hz, 1H), 8.53 (d, *J* = 9.2 Hz, 1H), 7.71 (d, *J* = 9.2 Hz, 1H), 7.65 (d, *J* = 9.2 Hz, 1H), 7.58–7.55 (m, 2H), 7.40 (d, *J* = 9.2 Hz, 1H), 7.36 (dd, *J* = 9.2 Hz, 2.0 Hz, 1H), 7.33–7.30 (m, 3H), 7.25 (dd, *J* = 9.2 Hz, 2.0 Hz, 1H), 7.23 (d, *J* = 2.0 Hz, 1H), 7.16 (d, *J* = 2.0 Hz, 1H), 6.95 (d, *J* = 2.0 Hz, 1H); ¹³C NMR (125 MHz, DMSO-*d*₆) δ 175.6, 173.6, 163.1, 162.7, 162.4, 159.2, 158.1, 158.0, 153.7, 153.3, 139.7, 138.4, 133.6, 131.8, 126.7, 126.0, 124.6, 123.7, 123.4, 122.9, 120.7, 120.3, 119.4, 117.6, 116.9, 116.6, 115.9, 115.4, 114.4, 113.6, 111.4, 110.1, 104.5, 103.0; HRMS (EI⁺, double-focusing magnetic sector) calcd for C₃₄H₁₉O₇ (M + H)⁺, 539.1123; found, 539.1131.

3,10-Dihydroxy-8-(8-hydroxy-3-oxo-benzo[*b*]xanthen-12-yl)-benzo[*c*]xanthen-7-one (18). Yield 86%; red powder; mp > 300 °C; IR (KBr) 3199, 2362, 1600, 1521, 1477, 1394, 1344, 1251, 1199, 1153, 1120 cm⁻¹; ¹H NMR (400 MHz, DMSO-*d*₆) δ 11.4 (s, 1H), 10.5 (s, 1H), 10.4 (s, 1H), 8.62 (d, *J* = 9.2 Hz, 1H), 7.82 (s, 1H), 7.74 (d, *J* = 9.2 Hz, 1H), 7.68 (d, *J* = 8.8 Hz, 1H), 7.59 (s, 1H), 7.58 (d, *J* = 8.8 Hz, 1H), 7.41 (d, *J* = 2.0 Hz, 1H), 7.36 (dd, *J* = 9.2 Hz, 2.4 Hz, 1H), 7.28 (d, *J* = 2.4 Hz, 1H), 7.21 (d, *J* = 2.0 Hz, 1H), 6.99 (d, *J* = 9.6 Hz, 1H), 6.99 (dd, *J* = 9.2 Hz, 2.4 Hz, 1H), 6.89 (d, *J* = 2.4 Hz, 1H), 6.32 (dd, *J* = 9.6 Hz, 2.0 Hz, 1H), 6.26 (d, *J* = 2.0 Hz, 1H); ¹³C NMR (125 MHz, DMSO-*d*₆) δ 184.7, 173.5, 162.4, 158.9, 158.2, 158.2, 158.0, 152.8, 150.7, 148.5, 138.2, 137.4, 134.5, 131.4, 131.1, 128.5, 128.5, 124.7, 124.5, 122.7, 120.9, 119.2, 118.9, 118.6, 117.8, 116.5, 116.2, 114.7, 113.7, 110.0, 109.6, 107.5, 105.0, 104.0; HRMS (FT-ICR-MS) calcd for C₃₄H₁₇O₇ (M-H)⁻, 537.0979; found, 537.0980.

■ ASSOCIATED CONTENT

📄 Supporting Information

A plausible reaction mechanism of the unexpected dimerization of xanthenone **1**. UV–vis and fluorescence spectra of dimeric dye **18** and its fragment molecules **21** and **23** and DFT calculations of the optimized structures of dimeric dyes **5**, **16**, and **18**. ¹H and ¹³C NMR spectra for all new compounds. This material is available free of charge via the Internet at <http://pubs.acs.org>.

■ AUTHOR INFORMATION

✉ Corresponding Author

*E-mail: tsubaki@kpu.ac.jp.

Notes

The authors declare no competing financial interest.

■ ACKNOWLEDGMENTS

The authors thank Prof. Akito Ishida (Kyoto Prefectural University) for useful suggestions and discussion. The authors also appreciate the assistance of Kyoko Ohmine (ICR, Kyoto

University) with NMR analysis and Sakiko Akaji, Dr. Yasushi Nakata, and Ikuko Hamagami (Horiba, Ltd.) with measurements of the fluorescence lifetimes of dimeric dyes. This study was partly supported by a Grant-in-Aid for the Japan Society for the Promotion of Science (JSPS) Fellows (to E.A.) and KAKENHI (nos. 22390003, 26293005, and 15K14931). This study was carried out using the 600 MHz NMR spectrometer and Fourier transform ion cyclotron resonance mass spectrometer at the Joint Usage/Research Center, Kyoto University.

REFERENCES

- (1) For recent reviews, see: (a) de Silva, A. P.; Gunaratne, H. Q. N.; Gunnlaugsson, T.; Huxley, A. J. M.; McCoy, C. P.; Rademacher, J. T.; Rice, T. E. *Chem. Rev.* **1997**, *97*, 1515–1566. (b) Loudet, A.; Burgess, K. *Chem. Rev.* **2007**, *107*, 4891–4932. (c) Kobayashi, H.; Ogawa, M.; Alford, R.; Choyke, P. L.; Urano, Y. *Chem. Rev.* **2010**, *110*, 2620–2640. (d) Kikuchi, K. *Chem. Soc. Rev.* **2010**, *39*, 2048–2053.
- (2) (a) Urano, Y.; Kamiya, M.; Kanda, K.; Ueno, T.; Hirose, K.; Nagano, T. *J. Am. Chem. Soc.* **2005**, *127*, 4888–4894. (b) Kamiya, M.; Kobayashi, H.; Hama, Y.; Koyama, Y.; Bernardo, M.; Nagano, T.; Choyke, P. L.; Urano, Y. *J. Am. Chem. Soc.* **2007**, *129*, 3918–3929. (c) Terai, T.; Tomiyasu, R.; Ota, T.; Ueno, T.; Komatsu, T.; Hanaoka, K.; Urano, Y.; Nagano, T. *Chem. Commun.* **2013**, *49*, 3101–3103.
- (3) (a) Mottram, L. F.; Boonyarattanakalin, S.; Kovel, R. E.; Peterson, B. R. *Org. Lett.* **2006**, *8*, 581–584. (b) Kim, S. H.; Gunther, J. R.; Katzenellenbogen, J. A. *Org. Lett.* **2008**, *10*, 4931–4934. (c) Wu, L.; Burgess, K. *J. Org. Chem.* **2008**, *73*, 8711–8718. (d) Li, J.; Hu, M.; Yao, S. Q. *Org. Lett.* **2009**, *11*, 3008–3011. (e) Woydziak, Z. R.; Fu, L.; Peterson, B. R. *J. Org. Chem.* **2012**, *77*, 473–481.
- (4) Azuma, E.; Kuramochi, K.; Tsubaki, K. *Tetrahedron* **2013**, *69*, 1694–1699.
- (5) Azuma, E.; Nakamura, N.; Kuramochi, K.; Sasamori, T.; Tokitoh, N.; Sagami, I.; Tsubaki, K. *J. Org. Chem.* **2012**, *77*, 3492–3500.
- (6) MOM-protected xanthenes were synthesized from corresponding dihydroxy xanthenes and MOMCl under basic conditions; see the Experimental Section.
- (7) (a) Abrams, S. R. *J. Labelled Compd. Radiopharm.* **1987**, *24*, 941–948. (b) Odrowaz-Sypniewski, M. R.; Tsoungas, P. G.; Varvounis, G.; Cordopatis, P. *Tetrahedron Lett.* **2009**, *50*, 5981–5983.
- (8) A plausible reaction mechanism is shown in Scheme S1.
- (9) For reports on energy transfer in orthogonally arranged chromophores, see: (a) Yoshida, N.; Ishizuka, T.; Osuka, A.; Jeong, D. H.; Cho, H. S.; Kim, D.; Matsuzaki, Y.; Nogami, A.; Tanaka, K. *Chem.—Eur. J.* **2003**, *9*, 58–75. (b) Rostron, J. P.; Ulrich, G.; Retaillieu, P.; Harriman, A.; Ziessel, R. *New J. Chem.* **2005**, *29*, 1241–1244. (c) Langhals, H.; Poxleitner, S.; Krotz, O.; Pust, T.; Walter, A. *Eur. J. Org. Chem.* **2008**, 4559–4562. (d) Langhals, H.; Esterbauer, A. J.; Walter, A.; Riedle, E.; Pugliesi, I. *J. Am. Chem. Soc.* **2010**, *132*, 16777–16782. (e) Du, Y.; Jiang, L.; Zhou, J.; Qi, G.; Li, X.; Yang, Y. *Org. Lett.* **2012**, *14*, 3052–3055.
- (10) (a) Mchedlov-Petrosyan, N. O.; Vodolazkaya, N. A.; Gurina, Y. A.; Sun, W.-C.; Gee, K. R. *J. Phys. Chem. B* **2010**, *114*, 4551–4564. (b) Martin, M. M.; Lindqvist, L. *J. Lumin.* **1975**, *10*, 381–390.
- (11) Frisch, M. J.; Trucks, G. W.; Schlegel, H. B.; Scuseria, G. E.; Robb, M. A.; Cheeseman, J. R.; Scalmani, G.; Barone, V.; Mennucci, B.; Petersson, G. A.; Nakatsuji, H.; Caricato, M.; Li, X.; Hratchian, H. P.; Izmaylov, A. F.; Bloino, J.; Zheng, G.; Sonnenberg, J. L.; Hada, M.; Ehara, M.; Toyota, K.; Fukuda, R.; Hasegawa, J.; Ishida, M.; Nakajima, T.; Honda, Y.; Kitao, O.; Nakai, H.; Vreven, T.; Montgomery, J. A., Jr.; Peralta, J. E.; Ogliaro, F.; Bearpark, M.; Heyd, J. J.; Brothers, E.; Kudin, K. N.; Staroverov, V. N.; Kobayashi, R.; Normand, J.; Raghavachari, K.; Rendell, A.; Burant, J. C.; Iyengar, S. S.; Tomasi, J.; Cossi, M.; Rega, N.; Millam, M. J.; Klene, M.; Knox, J. E.; Cross, J. B.; Bakken, V.; Adamo, C.; Jaramillo, J.; Gomperts, R.; Stratmann, R. E.; Yazyev, O.; Austin, A. J.; Cammi, R.; Pomelli, C.; Ochterski, J. W.; Martin, R. L.; Morokuma, K.; Zakrzewski, V. G.; Voth, G. A.; Salvador, P.; Dannenberg, J. J.; Dapprich, S.; Daniels, A. D.; Farkas, Ö.;
- Foresman, J. B.; Ortiz, J. V.; Cioslowski, J.; Fox, D. J. *Gaussian 09*, Revision D.01; Gaussian, Inc.: Wallingford, CT, 2009.
- (12) For compound **19**: (a) Šebej, P.; Wintner, J.; Müller, P.; Slanina, T.; Al Anshori, J.; Antony, L. A. P.; Klán, P.; Wirz, J. *J. Org. Chem.* **2013**, *78*, 1833–1843. For compound **20**: (b) Yang, Y.; Escobedo, J. O.; Wong, A.; Schowalter, C. M.; Touchy, M. C.; Jiao, L.; Crowe, W. E.; Fronczek, F. R.; Strongin, R. M. *J. Org. Chem.* **2005**, *70*, 6907–6912. For compounds **22** and **23**: (c) Yang, Y.; Lowry, M.; Xu, X. Y.; Escobedo, J. O.; Sibrian-Vazquez, M.; Wong, L.; Schowalter, C. M.; Jensen, T. J.; Fronczek, F. R.; Warner, I. M.; Strongin, R. M. *Proc. Natl. Acad. Sci. U.S.A.* **2008**, *105*, 8829–8834.
- (13) Lee, L. G.; Berry, G. M.; Chen, C.-H. *Cytometry* **1989**, *10*, 151–164.
- (14) (a) Lakowicz, J. R. Energy transfer. *Principles of Fluorescence Spectroscopy*, 2nd ed; Kluwer Academic/Plenum Publishers: New York, 1999; pp 367–393. (b) Steinberg, I. Z. *Annu. Rev. Biochem.* **1971**, *40*, 93–114. (c) Michalet, X.; Weiss, S.; Jäger, M. *Chem. Rev.* **2006**, *106*, 1785–1813.
- (15) *The Merck Index*, 13th ed.; Merck: Whitehouse Station, NJ, 2001; p 1065.
- (16) *The Merck Index*, 13th ed.; Merck: Whitehouse Station, NJ, 2001; p 1971.